

## Spectroscopy of odd-mass cobalt isotopes toward the $N = 40$ subshell closure and shell-model description of spherical and deformed states

F. Recchia,<sup>1,2</sup> S. M. Lenzi,<sup>1,2</sup> S. Lunardi,<sup>1,2</sup> E. Farnea,<sup>2</sup> A. Gadea,<sup>3,4</sup> N. Mărginean,<sup>4,5</sup> D. R. Napoli,<sup>4</sup> F. Nowacki,<sup>6</sup> A. Poves,<sup>7</sup> J. J. Valiente-Dobón,<sup>4</sup> M. Axiotis,<sup>4</sup> S. Aydin,<sup>2,8</sup> D. Bazzacco,<sup>2</sup> G. Benzoni,<sup>9</sup> P. G. Bizzeti,<sup>10</sup> A. M. Bizzeti-Sona,<sup>10</sup> A. Bracco,<sup>9,11</sup> D. Bucurescu,<sup>5</sup> E. Caurier,<sup>6</sup> L. Corradi,<sup>4</sup> G. de Angelis,<sup>4</sup> F. Della Vedova,<sup>4</sup> E. Fioretto,<sup>4</sup> A. Gottardo,<sup>1,4</sup> M. Ionescu-Bujor,<sup>5</sup> A. Iordachescu,<sup>5</sup> S. Leoni,<sup>9,11</sup> R. Mărginean,<sup>2,5</sup> P. Mason,<sup>1,2</sup> R. Menegazzo,<sup>2</sup> D. Mengoni,<sup>1,2</sup> B. Million,<sup>9</sup> G. Montagnoli,<sup>1,2</sup> R. Orlandi,<sup>4</sup> G. Pollarolo,<sup>12</sup> E. Sahin,<sup>4</sup> F. Scarlassara,<sup>1,2</sup> R. P. Singh,<sup>4</sup> A. M. Stefanini,<sup>4</sup> S. Szilner,<sup>13</sup> C. A. Ur,<sup>2</sup> and O. Wieland<sup>9</sup>

<sup>1</sup>*Dipartimento di Fisica, Università degli Studi di Padova, Padova, Italy*

<sup>2</sup>*INFN Sezione di Padova, Padova, Italy*

<sup>3</sup>*IFIC, CSIC—Universitat de València, València, Spain*

<sup>4</sup>*INFN Laboratori Nazionali di Legnaro, Legnaro, Italy*

<sup>5</sup>*Horia Hulubei National Institute of Physics and Nuclear Engineering, Bucharest, Romania*

<sup>6</sup>*IPHC, IN2P3-CNRS et Université de Strasbourg, Strasbourg, France*

<sup>7</sup>*Departamento de Física Teórica and IFT-UAM/CSIC, Universidad Autónoma de Madrid, Madrid, Spain*

<sup>8</sup>*Department of Physics, University of Aksaray, Aksaray, Turkey*

<sup>9</sup>*INFN Sezione di Milano, Milano, Italy*

<sup>10</sup>*Dipartimento di Fisica, Università and INFN Sezione di Firenze, Firenze, Italy*

<sup>11</sup>*Dipartimento di Fisica, Università di Milano, Milano, Italy*

<sup>12</sup>*Dipartimento di Fisica, Università and INFN Sezione di Torino, Torino, Italy*

<sup>13</sup>*Ruder Bošković Institute, Zagreb, Croatia*

(Received 28 March 2012; published 6 June 2012)

The neutron-rich cobalt isotopes up to  $A = 67$  have been studied through multinucleon transfer reactions by bombarding a  $^{238}\text{U}$  target with a 460-MeV  $^{70}\text{Zn}$  beam. Unambiguous identification of prompt  $\gamma$  rays belonging to each nucleus has been achieved using coincidence relationships with the ions detected in a high-acceptance magnetic spectrometer. The new data are discussed in terms of the systematics of the cobalt isotopes and interpreted with large-scale shell-model calculations in the *fpgd* model space. In particular, very different shapes can be described in  $^{67}\text{Co}$ , at the edge of the island of inversion at  $N = 40$ , where a low-lying highly deformed band coexists with a spherical structure.

DOI: [10.1103/PhysRevC.85.064305](https://doi.org/10.1103/PhysRevC.85.064305)

PACS number(s): 21.10.Re, 21.60.Cs, 23.20.Lv, 27.50.+e

### I. INTRODUCTION

New experimental information on neutron-rich nuclei has been provided by now on many regions of the nuclear chart, contributing to a unified description of the nuclear structure. A wealth of fascinating phenomena have been observed in the study of neutron-rich nuclei of the region bounded by  $N = 28$ –50 and  $Z = 20$ –28, such as new subshell closures [1,2], new regions of deformation [3,4], and islands of isomers [5]. One of the successful methods of accessing exotic neutron-rich nuclei in this region has been the use of multinucleon transfer and deep-inelastic reactions produced by the collisions of stable beams with stable targets [6]. With this method, the doubly-magic character of  $^{68}\text{Ni}$  at the neutron number  $N = 40$  has been suggested for the first time [1]. More recently, by coupling an efficient  $\gamma$ -ray array with a large-acceptance magnetic spectrometer for heavy-ion detection, we have extended these studies to the low- to medium-spin structure of many neutron-rich isotopes in this nuclear region [7–12]. For the majority of them, the only information available arose from  $\beta$ -decay studies, the knowledge of high-spin states being limited to less neutron rich nuclei, that could be produced in fusion-evaporation reactions. For the cobalt chain the most neutron rich nucleus whose high-spin structure is known from a fusion-reaction study is  $^{63}\text{Co}$  [13]. Here, we will present

results on more exotic cobalt isotopes, up to  $^{67}\text{Co}$ , produced in a multinucleon transfer reaction.

The cobalt nuclei have one  $f_{7/2}$  proton hole with respect to the  $Z = 28$  shell closure. The ground state of odd-mass cobalt isotopes has spin  $7/2^-$  and the excited states can be interpreted as the coupling of the  $f_{7/2}$  proton hole with the corresponding even-even nickel core excitations. In particular, a  $9/2^-$ - $11/2^-$  doublet appears at approximately the same excitation energy of the  $2^+$  state of the adjacent nickel neighbor, with the  $9/2^-$  state following more closely the  $2^+$  energy. These states are understood as the two high-spin members of the  $\pi f_{7/2}^{-1} \otimes 2^+(\text{Ni})$  multiplet. The  $9/2^-$ - $11/2^-$  states lie at  $\approx 3$  MeV in the  $N = 28$  nucleus  $^{55}\text{Co}$ , one proton hole with respect to doubly-magic  $^{56}\text{Ni}$  (where the  $2^+$  state is at 2.7 MeV) whereas they drop at an energy of 1.2 and 1.7 MeV, respectively, in  $^{57}\text{Co}$  (with the  $2^+$  of the  $^{58}\text{Ni}$  core being at 1.4 MeV). The presence of the  $N = 28$  shell closure is hence clearly evident in the excitation spectrum of Co isotopes. Furthermore,  $^{55}\text{Co}$  is the only odd-mass cobalt isotope where the ordering between the  $9/2^-$  and the  $11/2^-$  states is reversed. Even if by only 3 keV, the  $11/2^-$  state is lower in energy, in contrast to the other known odd-mass isotopes [14]. By adding neutrons, cobalt isotopes reach the subshell closure at  $N = 40$ . In  $^{68}\text{Ni}$  the  $2^+$  state lies at a significantly higher

energy (2.033 MeV) with respect to the adjacent even-even nickel isotopes [1]. We may therefore expect, as in the case of the  $N = 28$   $^{55}\text{Co}$ , that this shell closure shows its effects also in the cobalt nuclei approaching  $N = 40$ , i.e., the  $^{65}\text{Co}$  and  $^{67}\text{Co}$  nuclei, whose excited structure was very poorly known at the beginning of our study. In the meantime, new data on both nuclei appeared in the literature from  $\beta$ -decay experiments [15] and, in the case of  $^{65}\text{Co}$ , also from heavy-ion deep inelastic reactions [16,17].

It is also clear by now that the shell closure at  $N = 40$  disappears suddenly just by removing protons from  $^{68}\text{Ni}$ . According to the predictions of shell-model calculations, deformation appears as an effect of the interaction of neutrons excited to the  $gds$  shell with  $pf$  protons [18]. This happens, with increasing neutron number when approaching  $N = 40$ , in nuclei where the proton  $1f_{7/2}$  shell is not completely filled. In fact, according to experimental findings and calculations, the removal of two or four  $f_{7/2}$  protons from the spherical  $^{68}\text{Ni}$  drives the  $N = 40$  nuclei  $^{66}\text{Fe}$  and  $^{64}\text{Cr}$  into prolate shapes, generating a new region of deformation [18,19]. This has been indeed proven subsequently by various experiments [3,4,8,20–22]. The  $^{65,67}\text{Co}$  nuclei, with one proton less than the spherical nickel isotopes and one proton more than the deformed iron isotopes, may show both shapes coexisting in their level structure. Indeed, a deformed  $(1/2^-)$  proton-intruder state has been recently reported at low energy in  $^{67}\text{Co}$ , suggesting the washing out, as in iron and chromium isotopes, of the  $N = 40$  shell gap [15]. On the other side, the  $9/2^- - 11/2^-$  states, which may still indicate the presence of the  $N = 40$  gap, were not known in  $^{65,67}\text{Co}$  and their identification was one of the purposes of the present study.

In order to address these questions, we have studied the neutron-rich  $^{65,67}\text{Co}$  isotopes through the multinucleon transfer reaction  $^{70}\text{Zn} + ^{238}\text{U}$  at the Laboratori Nazionali di Legnaro using the the CLARA-PRISMA setup [23,24]. In this paper we present our results on prompt  $\gamma$  rays belonging to all neutron-rich cobalt nuclei produced in the reaction. In Sec. II the new experimental data for all the cobalt isotopes from  $A = 61$  to  $A = 67$  are illustrated. The level schemes of the odd-even cobalt isotopes are then interpreted in Sec. III by means of state-of-the-art shell-model calculations.

## II. EXPERIMENTS AND RESULTS

The neutron-rich cobalt isotopes were populated as products of a multinucleon transfer process following the collision of a  $^{70}\text{Zn}$  beam onto a  $^{238}\text{U}$  target. The  $^{70}\text{Zn}$  beam, with an energy of 460 MeV, was delivered by the Laboratori Nazionali di Legnaro (LNL) Tandem-ALPI accelerator complex. The thickness of the uranium target was  $400 \mu\text{g}/\text{cm}^2$ . The CLARA-PRISMA setup has been used to identify the projectile-like nuclei in coincidence with the prompt  $\gamma$  rays emitted from their excited states. The PRISMA large-acceptance magnetic spectrometer was positioned at  $64^\circ$ , close to the grazing angle. The  $\gamma$  rays following the de-excitation of the reaction products were detected with the CLARA array, in a configuration with 22 Compton-suppressed Ge clover detectors. CLARA was positioned in the hemisphere opposite to the PRISMA

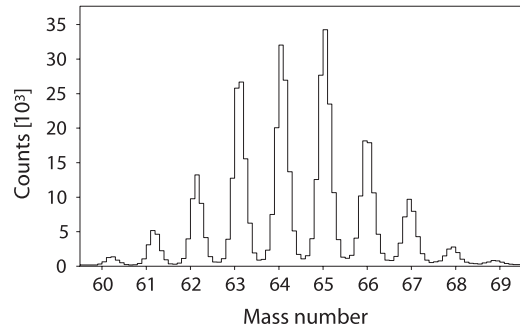


FIG. 1. Mass spectrum of cobalt isotopes detected at the focal plane of the PRISMA spectrometer following the  $^{70}\text{Zn} + ^{238}\text{U}$  reaction at 460 MeV.

spectrometer, covering the polar angles from  $98^\circ$  to  $180^\circ$ . Doppler correction of  $\gamma$  rays was performed on an event-by-event basis. The efficiency of the CLARA spectrometer was 2.5%. More details on the CLARA-PRISMA setup and data analysis used for the present experiment can be found in Refs. [8,25,26]. Clean mass spectra were obtained for all the isotope chains populated in the  $^{70}\text{Zn}$ -induced reaction. We will concentrate here on the  $-3p$   $xn$  transfer channels, leading to the cobalt isotopes. The mass spectrum obtained for the cobalt isotopes is shown in Fig. 1. The most populated nuclei are  $^{64}\text{Co}$  and  $^{65}\text{Co}$  in the  $-3p-3n$  and  $-3p-2n$  transfer channels, respectively. Neutron-rich cobalt isotopes up to  $^{67}\text{Co}$  are produced with sufficient yield to enable recoil- $\gamma$  coincidence measurements. The  $\gamma$ -ray spectra obtained in coincidence with the detection of odd-even cobalt isotopes from  $A = 61$  to  $A = 67$  are shown in Fig. 2. This allows the assignment, in some cases for the first time, of  $\gamma$  rays to a specific nucleus. The statistics of the  $\gamma$ - $\gamma$  data of CLARA was not sufficient to establish coincidence relationships among the  $\gamma$  rays assigned to each isotope, except for the less exotic case of  $^{63}\text{Co}$  and  $^{64}\text{Co}$ . In particular, in  $^{63}\text{Co}$  coincidence relationships are observed between the 191-, 356-, and 495-keV  $\gamma$  rays, in agreement with the level scheme proposed in Ref. [13]. In  $^{64}\text{Co}$  a coincidence relationship is observed between the two newly observed  $\gamma$  rays of 274 and 738 keV.

As stated above, the CLARA detectors were covering angles from  $98^\circ$  to  $180^\circ$  and therefore the angular distribution of the  $\gamma$ -ray transitions could be analyzed. In particular, we have extracted the anisotropy ratio

$$R_{\text{ASYM}} = \frac{I_\gamma(\theta \geq 150^\circ)}{I_\gamma(\theta = 100^\circ)}, \quad (1)$$

i.e., the intensity of a given transition measured in the detectors covering the backward angles (with  $\theta$  in the  $150^\circ$ – $180^\circ$  range) divided by the intensity of the same  $\gamma$  ray detected in the ring of detectors placed at  $\theta = 100^\circ$ . In Table I, such a ratio is reported after proper normalization for known  $\gamma$ -ray transitions in the nuclei  $^{64,66}\text{Ni}$  and  $^{62}\text{Fe}$  populated in the same reaction. The statistics are not very good and consequently the errors on  $R_{\text{ASYM}}$  are large, but nevertheless one can conclude that stretched  $\Delta I = 1$  transitions have  $R_{\text{ASYM}} \approx 0.8$ , whereas stretched  $\Delta I = 2$  transitions have  $R_{\text{ASYM}} \approx 1.2$  or larger. This is consistent with recent angular distribution

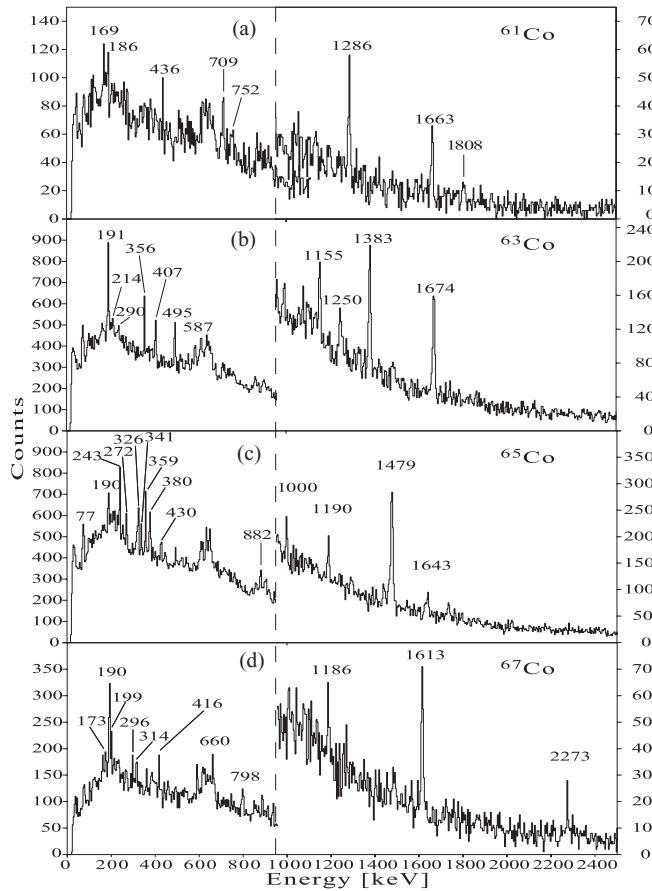


FIG. 2. Doppler-corrected  $\gamma$ -ray spectra in coincidence with the four odd-mass cobalt recoils discussed in this work. Transitions assigned to each nucleus are labeled by their energies.

results obtained with CLARA in a similar reaction [12,27]. Where better statistics are available, we have then measured the anisotropy ratios for transitions belonging to the cobalt nuclei and used them to assign multiplicities. Table II summarizes the results obtained, for the cobalt nuclei, from the CLARA-PRISMA experiment. The  $\gamma$ -ray transitions, their relative intensities (normalized sums of the intensities measured at the different counters), the anisotropy ratios, and the tentative spin assignment for the levels involved are given.

We have subsequently performed another multinucleon transfer experiment with the main goal to establish coincidence relationships among transitions in cobalt isotopes. For this purpose we have bombarded a  $40 \text{ mg/cm}^2$   $^{208}\text{Pb}$  target on a  $20 \text{ mg/cm}^2$   $^{197}\text{Au}$  backing with a  $^{70}\text{Zn}$  beam at 460 MeV. In this case, the GASP array [28] was used to collect  $\gamma$ - $\gamma$  coincidences. Such reactions lead to the production of a wide range of target-like and projectile-like fragments and the resulting  $\gamma$ -ray spectra are very complex. The cobalt nuclei are furthermore weakly populated so that  $\gamma$ - $\gamma$ -coincidences are not clean enough for a meaningful analysis. By using triple coincidence data, useful information could be obtained only for the strongest Co channels,  $^{63,65}\text{Co}$ .

The experimental results will be discussed in the following sections.

TABLE I. Energies, relative intensities, and anisotropy parameters of known  $\gamma$  transitions of some even-even nuclei populated in the reaction. The spin assignments of the levels involved in the transition are taken from the literature.

$E_\gamma$ (keV)	$I_\gamma$	$R_{\text{ASYM}}$	$J_i^\pi \rightarrow J_f^\pi$
$^{62}\text{Fe}$			
838.7(3)	34(3)	0.75(20)	$(5^-) \rightarrow (4^+)$
877.8(2)	100(4)	1.13(12)	$2^+ \rightarrow 0^+$
1210.6(4)	32(3)	1.58(35)	$(6^+) \rightarrow (4^+)$
1299.0(2)	83(5)	1.77(23)	$(4^+) \rightarrow 2^+$
$^{64}\text{Ni}$			
1239.9(3)	37(2)	0.94(13)	$5^- \rightarrow 4^+$
1264.0(2)	54(3)	1.19(13)	$4^+ \rightarrow 2^+$
1345.1(2)	100(3)	1.21(10)	$2^+ \rightarrow 0^+$
$^{66}\text{Ni}$			
490.2(2)	35(1)	0.82(7)	$7^- \rightarrow 6^-$
1425.0(1)	100(2)	1.83(11)	$2^+ \rightarrow 0^+$
1758.2(3)	34(2)	2.14(28)	$4^+ \rightarrow 2^+$

### A. The $^{61,63}\text{Co}$ isotopes

The  $^{61,63}\text{Co}$  isotopes have been studied previously in a fusion-evaporation reaction and their excited states are known up to spin  $(17/2^-)$  and  $(19/2^-)$ , respectively [13]. Our data do not bring new information on these nuclei but we present them here with the purpose of showing which excited states, with the associated relative intensities, are populated in this multinucleon transfer reaction. These two cobalt nuclei are representative of the many other nuclei (e.g., nickel and copper isotopes) measured in our experiment and whose level schemes are well established. A common feature in all these nuclei is the strong population of the yrast states compared with a weak population of nonyrast ones. This observation will be very important for the interpretation in terms of spin assignment of the  $9/2^-$  and  $11/2^-$  states in  $^{65}\text{Co}$  and  $^{67}\text{Co}$  (see the next sections).

Figures 2(a) and 2(b) show the  $\gamma$ -ray spectra from CLARA in coincidence with  $^{61,63}\text{Co}$ . In  $^{63}\text{Co}$  we observe almost all the transitions assigned to the nucleus up to spin  $(19/2^-)$ . In  $^{61}\text{Co}$  the statistics are poorer but we clearly observe the transition de-exciting the high-lying state with spin  $(17/2^-)$ . This confirms that in this kind of reaction yrast and near-yrast states are populated. Figures 3 and 4 report the partial level schemes of  $^{61,63}\text{Co}$  (from Ref. [13]) with the relative  $\gamma$ -ray intensities observed in our multinucleon transfer reaction. The two spectra of Figs. 2(a) and 2(b) are dominated by the two high-energy transitions de-exciting the  $9/2^-$  and  $11/2^-$  states, respectively, to the  $7/2^-$  ground state. The  $9/2^-$  state, which in both nuclei lies a few hundred keV below the  $11/2^-$  state, is populated, within errors, with the same intensity as the  $11/2^-$  state. The different multipolarity character of the two transitions de-exciting the  $9/2^-$  and  $11/2^-$  states in  $^{63}\text{Co}$  ( $M1 + E2$  and  $E2$ , respectively) is confirmed by the anisotropy ratio measured for the 1383- and 1674-keV transitions (see Table II).

TABLE II. Energies and relative intensities of the  $\gamma$  transitions observed in coincidence with the cobalt isotopes. The anisotropy parameter of the angular distribution is reported together with the spin assignment of the levels involved in the transition. Asterisks (\*) mark the newly observed transitions.

$E_\gamma$ (keV)	$I_\gamma$	$R_{\text{ASYM}}$	$J_i^\pi \rightarrow J_f^\pi$
$^{61}\text{Co}$			
168.7(12)*	18(6)		
186.4(5)	18(4)		$(15/2^-) \rightarrow (13/2^-)$
436.1(9)	20(7)		$(17/2^-) \rightarrow (15/2^-)$
709.4(7)	45(9)		$(13/2^-) \rightarrow 11/2^-$
752.2(11)	42(15)		$(15/2^-) \rightarrow (13/2^-)$
1286.4(9)	100(15)		$(9/2^-) \rightarrow 7/2^-$
1663.5(5)	84(16)		$11/2^- \rightarrow 7/2^-$
1807.8(15)	40(10)		$(13/2^-) \rightarrow 11/2^-$
$^{62}\text{Co}$			
230.3(3)*	27(4)		
247.0(3)*	17(3)	0.60(33)	
309.3(15)*	17(5)		
326.7(2)	70(6)	1.24(25)	
588.2(3)	61(7)		$5^+ \rightarrow 5^+$
607.8(8)	15(7)		$(6^+) \rightarrow 5^+$
767.4(5)	40(7)		
889.4(10)*	26(7)		
1194.7(4)	100(10)	0.84(19)	$(6^+) \rightarrow 5^+$
$^{63}\text{Co}$			
191.2(2)	33(2)	0.98(18)	$(15/2^-) \rightarrow (13/2^-)$
214.3(16)*	5(3)		
290.3(5)	9(2)		$(11/2^-) \rightarrow (9/2^-)$
356.2(3)	31(3)		$(17/2^-) \rightarrow (15/2^-)$
407.1(3)	29(4)	0.97(28)	
495.1(4)	41(4)		$(13/2^-) \rightarrow (11/2^-)$
587.2(4)	32(9)	0.97(28)	$(19/2^-) \rightarrow (17/2^-)$
1155.5(4)	50(5)		$(11/2^-) \rightarrow (9/2^-)$
1249.8(12)	53(8)		
1383.0(4)	100(7)	1.02(26)	$(9/2^-) \rightarrow 7/2^-$
1673.9(4)	100(8)	1.43(23)	$(11/2^-) \rightarrow 7/2^-$
$^{64}\text{Co}$			
96.3(2)	59(4)	0.73(14)	$(4^+) \rightarrow (3^+)$
231.1(2)	59(3)	1.33(18)	$(3^+) \rightarrow (2^+, 3^+)$
274.1(2)*	100(4)	1.41(14)	
310.9(5)	17(3)		
341.3(6)	23(4)		
439.3(3)	37(4)		$(2^+, 3^+) \rightarrow (1^+)$
672.3(4)	37(8)		
738.5(2)*	85(6)	0.84(16)	
$^{65}\text{Co}$			
76.7(4)*	60(6)		
190.5(3)	9(1)	0.67(29)	$(13/2^-) \rightarrow (11/2^-)$
242.7(2)	15(2)	0.94(26)	$(15/2^-, 17/2^+) \rightarrow (15/2^-)$
272.4(5)*	10(2)		
325.6(3)*	17(2)		
340.7(7)	7(2)		$(3/2^-) \rightarrow (3/2^-)$
359.3(2)	18(2)		$(15/2^-) \rightarrow (13/2^-)$
379.7(4)*	18(2)		
430.1(6)*	6(2)		
882.3(7)	21(5)		$(3/2^-) \rightarrow (7/2^-)$
1000.4(6)	16(3)		$(11/2^-) \rightarrow (11/2^-)$

TABLE II. (*Continued.*)

$E_\gamma$ (keV)	$I_\gamma$	$R_{\text{ASYM}}$	$J_i^\pi \rightarrow J_f^\pi$
1190.5(9)	21(3)		$(13/2^-) \rightarrow (11/2^-)$
1479.5(3)	100(5)	1.19(14)	$(11/2^-) \rightarrow (7/2^-)$
1642.8(7)	14(3)		$(9/2^-) \rightarrow (7/2^-)$
$^{66}\text{Co}$			
165.7(2)*	36(3)	1.28(28)	
175.3(4)	26(4)		
182.8(2)*	100(5)	1.06(14)	
252.8(2)	47(5)	1.35(31)	
294.8(3)*	28(5)		
755.4(4)*	77(9)		
$^{67}\text{Co}$			
172.9(6)*	10(3)		
190.2(4)	46(4)	1.15(34)	$(5/2^-, 3/2^-) \rightarrow (1/2^-)$
199.1(3)*	13(3)		
295.9(9)*	11(4)		
314.0(7)*	19(4)		
415.8(5)*	17(4)		
659.7(7)*	19(6)		$(9/2^-) \rightarrow (11/2^-)$
797.9(5)*	22(5)		
1186.2(12)*	35(7)		$(13/2^-) \rightarrow (11/2^-)$
1612.7(7)*	100(10)	1.77(43)	$(11/2^-) \rightarrow (7/2^-)$
2273.1(20)*	31(6)		$(9/2^-) \rightarrow (7/2^-)$

### B. The $^{65}\text{Co}$ isotope

From  $\beta$ -decay studies a spin-parity of  $(7/2^-)$  was assigned to the  $^{65}\text{Co}$  ground state (g.s.) [29]. This  $(7/2^-)$  assignment is consistent with the systematics of the lighter odd-mass cobalt isotopes. The excited structure in  $^{65}\text{Co}$  has been investigated, in parallel with our work, by  $\beta^-$  decay of  $^{65}\text{Fe}$  and multinucleon transfer [16]. The  $\beta^-$  decay proceeds from the ground state of  $^{65}\text{Fe}$  as well as from an isomeric  $9/2^+$  state, reported at an excitation energy of 402 keV in a recent mass measurement [30]. The tentative spin-parity assignment to the excited states of  $^{65}\text{Co}$  proposed in Ref. [16] derives from the  $\log(ft)$  values measured separately from the decay of the g.s. and isomeric state of  $^{65}\text{Fe}$ . In particular, spin-parity of  $9/2^-$  and  $11/2^-$  have been proposed for the states at 1479 and 1643 keV, respectively, in  $^{65}\text{Co}$ . The  $\log(ft)$  values of the two states are equal within the errors, so that we can safely say that systematics arguments were the main reason to assign, as in the lighter odd Co isotopes,  $9/2^-$  to the state lying lower in energy and  $11/2^-$  to the one lying higher.

The  $\gamma$ -ray spectrum in coincidence with  $^{65}\text{Co}$  from our data is shown in Fig. 2(c); the intensities of the  $\gamma$  transitions observed in that spectrum are given in Table II. We observe the 1479- and 1643-keV transitions depopulating the states with spin  $9/2^-$  and  $11/2^-$ , respectively, as proposed from the  $\beta$ -decay data: their intensity ratio is however completely different from that measured for the two corresponding transitions in  $^{61,63}\text{Co}$ . This change of intensity is immediately evident from the comparison of Fig. 2(c) with Figs. 2(a) and 2(b). In  $^{65}\text{Co}$ , the lower energy transition (1479 keV), instead of having the same intensity, is seven times stronger than the high-energy one (1643 keV). Furthermore, the anisotropy ratio measured for the 1479-keV transition (see Table II) suggests a  $\Delta I = 2$

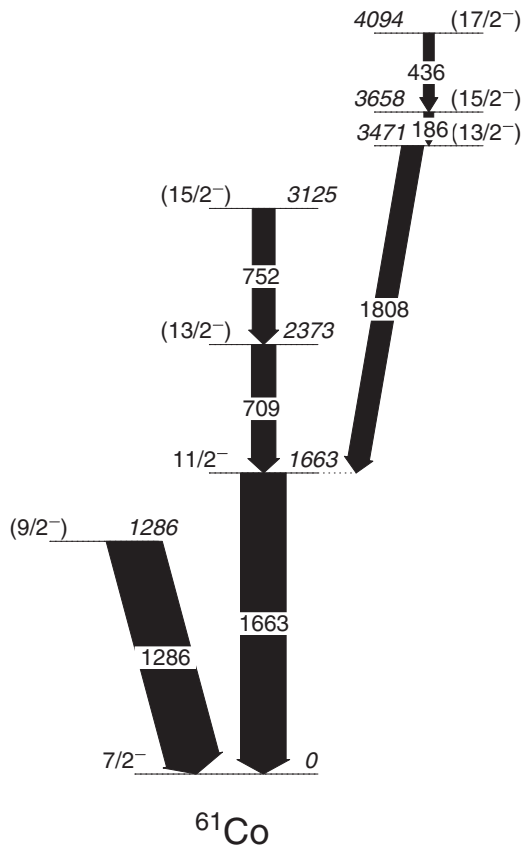


FIG. 3. Partial level scheme of  $^{61}\text{Co}$  from Ref. [13]. The width of the  $\gamma$ -ray transitions corresponds to the relative intensities observed in the present experiment.

character and therefore a spin  $11/2^-$  for the 1479-keV state. The level at 1643 keV would then have spin  $9/2^-$ . Such spin-parity inversion between the two high-spin members of the  $\pi f_{7/2}^{-1} \otimes 2^+$  ( $^{66}\text{Ni}$ ) multiplet can well explain the sudden change of relative population of the two states when going from  $^{61,63}\text{Co}$  to  $^{65}\text{Co}$ . If the  $9/2^-$  state is moved above the  $11/2^-$  in  $^{65}\text{Co}$ , becoming no longer yrast, its population will be unfavored, in agreement with our findings.

With the data of our thick-target experiment at GASP, we could establish coincidence relationships among some of the strong transitions: a summed doubly-gated coincidence spectrum is shown in Fig. 5. The level scheme of Fig. 6, which agrees with that of Ref. [16], is the result of such an analysis. The spins of states above 2 MeV are based on systematics.

### C. The $^{67}\text{Co}$ isotope

The only information available for the nucleus  $^{67}\text{Co}$  comes from  $\beta$ -decay experiments. The ground state is assumed to have spin  $7/2^-$  dominated by the  $\pi f_{7/2}^{-1}$  proton-hole configuration. Excited states in  $^{67}\text{Co}$  have been identified in an experiment [15,16] performed at the LISOL facility by selecting the products of proton-induced fission of  $^{238}\text{U}$ . A  $1/2^-$  isomeric state with a lifetime of 496(33) ms has been reported at an excitation energy of 492 keV which

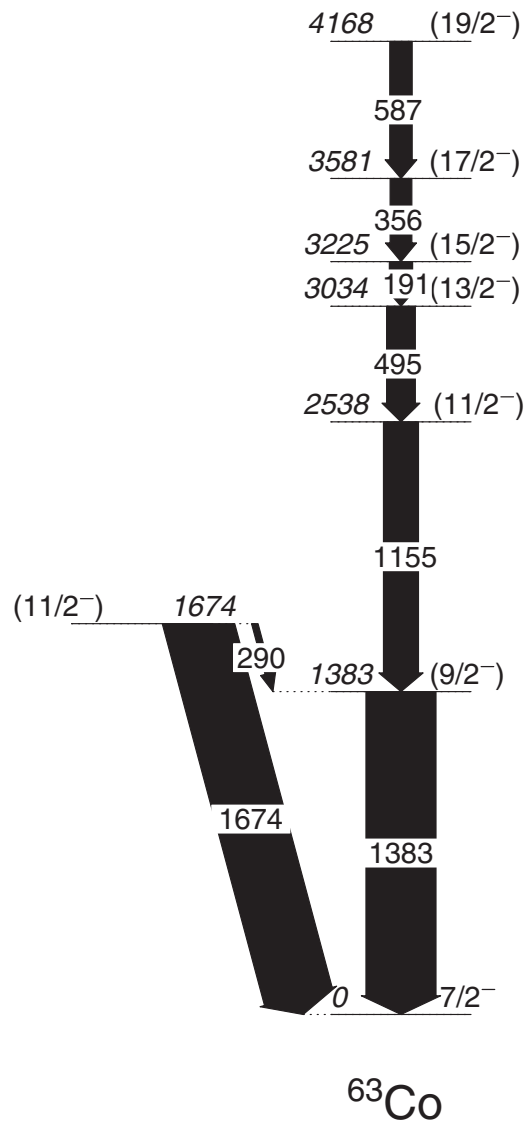


FIG. 4. Partial level scheme of  $^{63}\text{Co}$  from Ref. [13]. The width of the  $\gamma$ -ray transitions corresponds to the relative intensities observed in the present experiment.

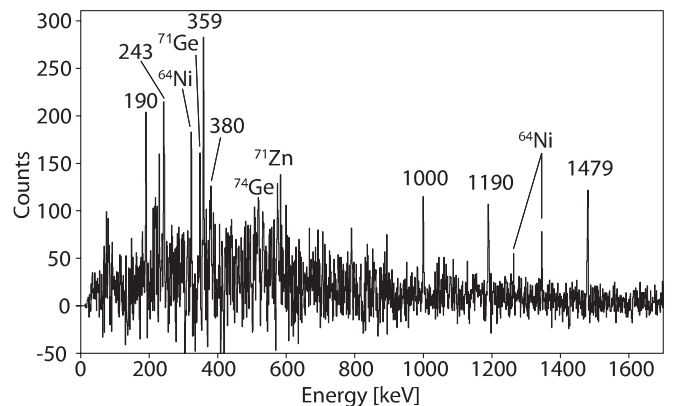


FIG. 5. Coincidence  $\gamma$ -ray spectrum for  $^{65}\text{Co}$  obtained in the thick-target GASP experiment using double gates on transitions of the nucleus. The spectrum is the sum of double gates on the transitions of energy 190, 243, 359, 1190, and 1479 keV.

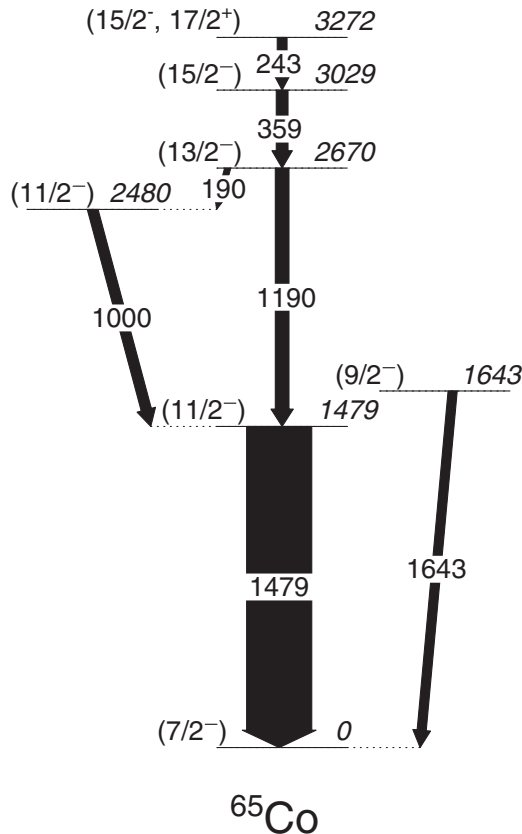


FIG. 6. Level scheme of  $^{65}\text{Co}$  from the data of the present experiment. The width of the  $\gamma$ -ray transitions corresponds to the relative intensities observed in the present experiment.

de-excites directly to the ground state with an  $M3$  transition. The configuration of this state is interpreted as a proton in the intruder  $[321]1/2^-$  Nilsson orbital which crosses the  $Z = 28$  gap at sizable deformation. Other low-spin excited states were populated in the  $\beta$  decay of  $^{67}\text{Fe}$  up to an excitation energy of  $\approx 2.8$  MeV.

The  $\gamma$ -ray spectrum in coincidence with  $^{67}\text{Co}$  from our PRISMA-CLARA data is shown in Fig. 2(d); the strongest transitions have energies of 190, 1186, 1613, and 2273 keV. Only the 190-keV transition was known before as feeding the  $1/2^-$  isomer [15].

From the angular distribution data we could obtain a  $R_{\text{ASYM}}$  value only for the strongest transition of 1613 keV. Its value (see Table II) of  $R_{\text{ASYM}} = 1.77(43)$  strongly suggests a stretched quadrupole character. As in the other odd-mass cobalt isotopes (see above  $^{61,63,65}\text{Co}$ ), we assume that such a high-energy transition feeds directly the  $7/2^-$  ground state, de-exciting one of the two high-spin members ( $9/2^-$  or  $11/2^-$ ) of the  $\pi f_{7/2}^{-1} \otimes 2^+$  multiplet. Because of the angular distribution results,  $J^\pi = 11/2^-$  is proposed for the 1613-keV excited state. The  $9/2^-$  state, decaying to the  $7/2^-$  ground state, is also expected to be reasonably populated. The only two transitions candidates for the  $9/2^- \rightarrow 7/2^-$  decay remain those at 1186 and 2273 keV. From energy level systematics of the lighter odd-even cobalt isotopes, the preferred population of yrast states in multinucleon transfer reactions and the

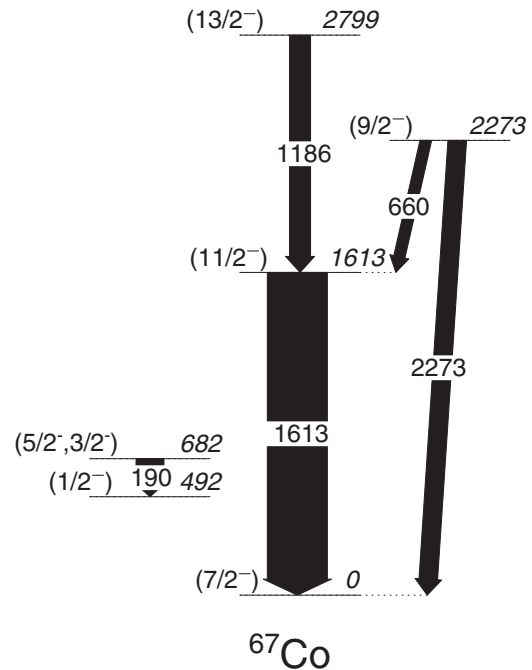


FIG. 7. Level scheme of  $^{67}\text{Co}$  from the data of the present experiment. The width of the  $\gamma$ -ray transitions corresponds to the relative intensities observed in the present experiment. The isomeric  $1/2^-$  level at 492 keV is taken from [15].

relative intensities of the 1186- and 2273-keV transitions, it is most likely that the 2273-keV transition depopulates the  $9/2^-$  state and that the 1186-keV transition feeds the  $11/2^-$  state at 1613 keV. Additional support for this decay scheme comes from the observation of a weak transition at 660 keV whose energy is matching the difference between the 2273- and 1613-keV levels. We mention also that the 1186-keV transition feeding, in our proposed level scheme, the  $11/2^-$  state has almost the same energy (1190 keV) of the corresponding transition in  $^{65}\text{Co}$ . From all these arguments, a level scheme is proposed for  $^{67}\text{Co}$ , shown in Fig. 7. The energy inversion of the  $9/2^-$ - $11/2^-$  states is also consistent with the relative intensities of the transitions depopulating the two levels. As in  $^{65}\text{Co}$ , the transition de-exciting the nonyrast  $9/2^-$  state is much weaker than that de-exciting the yrast  $11/2^-$  state (see Table II). Spin-parity of  $(13/2^-)$  is assigned to the 2799-keV level just on the basis of systematics.

#### D. The odd-odd cobalt isotopes

The odd-odd cobalt isotopes are also well populated in the  $^{70}\text{Zn} + ^{238}\text{U}$  reaction (see Fig. 1). In Table II we report the information obtained on  $\gamma$  rays observed in coincidence with  $^{62}\text{Co}$ ,  $^{64}\text{Co}$ , and  $^{66}\text{Co}$ . In  $^{62}\text{Co}$  excited states up to spin 8 are known from a fusion-evaporation reaction [31]. We see all the transitions de-exciting those states. Four new low-energy transitions are also in coincidence with  $^{62}\text{Co}$  recoils: they are marked with asterisks in Table II.

A  $(5^+)$  isomer with a half-life of 6.4 ns was reported [32] in  $^{64}\text{Co}$ , decaying toward the  $(1^+)$  ground state through seven

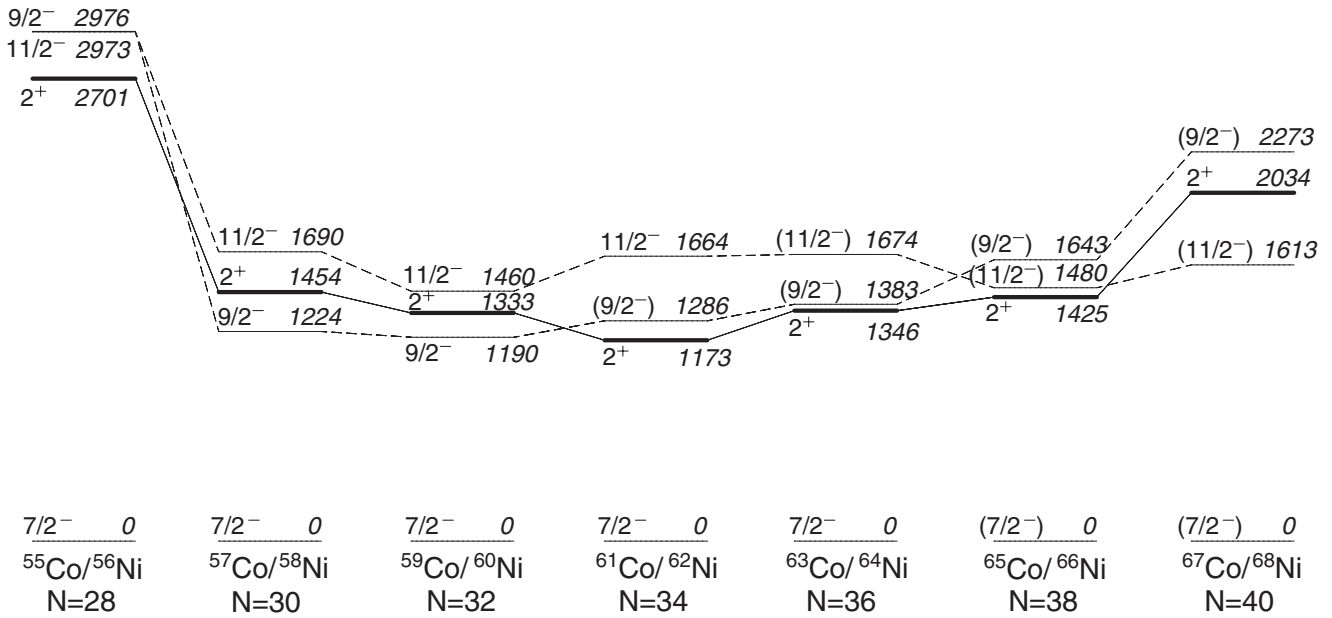


FIG. 8. Systematics of the first excited  $9/2^-$  and  $11/2^-$  states in the odd-even Co isotopes compared with the  $2^+$  levels in their respective nickel isotone.

$\gamma$  transitions. Beside the two isomeric ones, that, as expected, escape detection in CLARA, and the 329-keV transition that is reported to be very weak in Ref. [32], all the other transitions previously reported are clearly observed. Three transitions are new, among them the two most intense ones (274 and 738 keV) are also in mutual coincidence.

Two microsecond isomers were identified in  $^{66}\text{Co}$  in a fragmentation reaction [5]. Three transitions were also reported, with two of them being the isomeric ones, a 252-keV  $M2$  transition de-exciting the high-lying isomer with  $T_{1/2} > 100 \mu\text{s}$  and a 175-keV  $E2$  transition de-exciting the low-lying isomer with  $T_{1/2} = 1.21 \mu\text{s}$ . Our data disagree with the tentative decay pattern of Ref. [5] since we do observe both the isomeric transitions but not the third one at 214 keV, which, in that scheme, decays from an intermediate, nonisomeric level. To be compatible with our data, the transition depopulating the upper isomer has to be the 214-keV one, followed by the 252-keV transition. The presence of the 175-keV transition in our prompt spectrum implies the existence of a low-energy, unobserved transition as the one de-exciting the low-lying isomer.

Four new transitions are also identified to belong to  $^{66}\text{Co}$ . The two most intense ones (at 183 and 755 keV) resemble very much the two most intense ones observed in coincidence with  $^{64}\text{Co}$ , suggesting a similar decay sequence for the two nuclei. To understand the structure of these nuclei,  $\gamma$ - $\gamma$ -coincidence data from high-efficiency  $\gamma$  arrays are essential.

### III. DISCUSSION

As pointed out in the introduction, the level schemes of the odd-mass cobalt isotopes can be interpreted, to a first approximation, as a proton  $f_{7/2}$  hole coupled to the excited states of the neighboring spherical even-even nickel cores.

This is particularly evident for the  $9/2^-$ - $11/2^-$  doublet, whose energy, as shown in Fig. 8, follows quite closely the  $2^+$  state of the corresponding nickel isotope. However, the presence of a  $1/2^-$  state at very low excitation energy in  $^{67}\text{Co}$ , which is possible only in the hypothesis of a sizable deformation, cannot be directly deduced from such a comparison with  $^{68}\text{Ni}$ . The experimental results suggest the coexistence, in the same energy range, of states with very different structure: spherical nature for the  $9/2^-$ - $11/2^-$  doublet and a deformed one for the intruder  $1/2^-$  state. The simultaneous theoretical description, within a single formalism or model, of such structures is very challenging. The nuclear shell model has been demonstrated to be able to reproduce deformed structures provided an appropriate, large valence space [33] is considered. Such an approach has been successfully applied recently to describe the low-spin structure of even-mass chromium, iron, and nickel isotopes using a new effective interaction based on renormalized realistic interactions and monopole corrections in the model space consisting on the full  $pf$  shell for the protons and the  $p_{3/2}$ ,  $p_{1/2}$ ,  $f_{5/2}$ ,  $g_{9/2}$ , and  $d_{5/2}$  orbits for the neutrons, the LNPS interaction [19]. It has been shown that only with the inclusion of both the neutron  $g_{9/2}$  and  $d_{5/2}$  orbitals [a quasi-SU(3) space] it is possible to obtain the correlations necessary for the development of the island of inversion around  $^{64}\text{Cr}$ .

In the present work we interpret the data by means of large-scale shell-model calculations using the LNPS interaction.<sup>1</sup>

<sup>1</sup>The LNPS interaction used for the calculation presented in this work has some minor modifications with respect to the interaction used in Ref. [19]. Such differences are irrelevant around  $N = 40$  but improve the agreement with the experimental information toward  $N = 50$ .

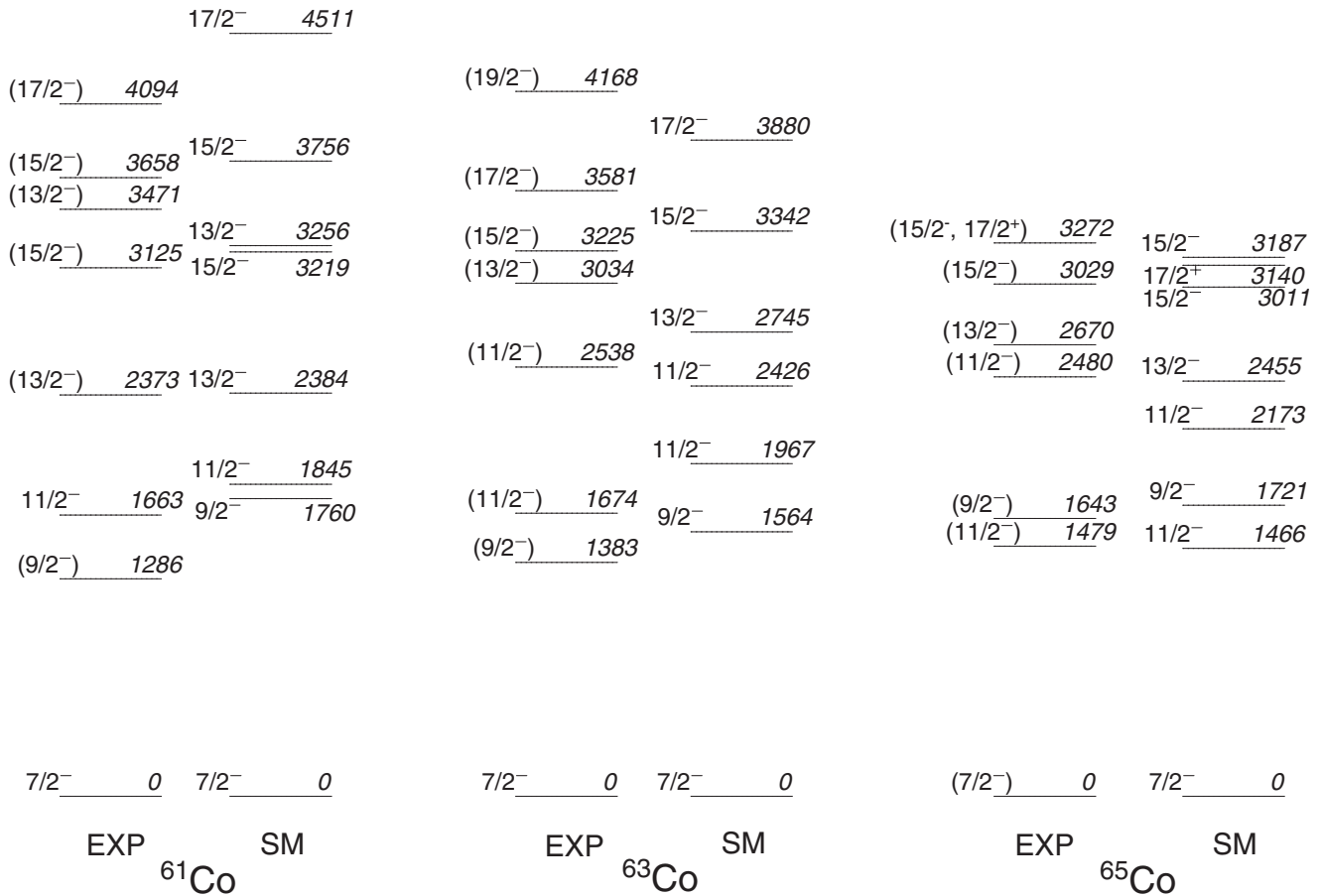


FIG. 9. Comparison of the experimental level schemes of the  $^{61,63,65}\text{Co}$  nuclei with the results of large-scale shell-model calculations using the LNPS interaction. The valence spaces change between  $^{63}\text{Co}$  and  $^{65}\text{Co}$  (see text for the details).

The lightest odd-mass cobalt isotope studied here is  $^{61}\text{Co}$ , whose yrast states can be interpreted as the coupling of the  $f_{7/2}$  proton hole to the yrast states of  $^{62}\text{Ni}$ . The highest observed state,  $17/2^-$  at 4094 keV, arising from the  $\pi f_{7/2}^{-1} \otimes 6^+$  coupling, decays through the yrare sequence  $15/2^- - 13/2^-$  to the yrast level with  $J^\pi = 11/2^-$ . This nucleus lies in the transitional region where the  $pf$  shell ends and the inclusion of the  $g_{9/2}$  orbital in the calculation becomes compulsory. In order to assess this transition, we have compared the  $fpgd$  and the  $pf$  valence spaces. The  $fpgd$  calculation shows that excitations to the  $g_{9/2}$  and  $d_{5/2}$  orbitals are negligible for all low-lying states whereas the  $pf$  calculation shows that neutron  $f_{7/2}$  excitations amount up to 50% of the  $17/2^-$  yrast state. Therefore  $^{40}\text{Ca}$  is taken as a core for  $^{61}\text{Co}$  and no excitations are allowed to the  $gd$  shell. The results of the calculations performed within this latter space are compared in Fig. 9 with the experimental results. The agreement is rather good and there is a one-to-one correspondence between all observed and calculated states.

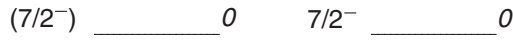
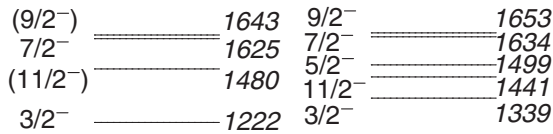
In  $^{63}\text{Co}$  the states associated with the coupling of the proton  $f_{7/2}$  hole to the yrast states of  $^{64}\text{Ni}$  are well reproduced by the shell-model calculations, as shown in Fig. 9. The highest observed state, with a spin assignment of  $(19/2^-)$  from Ref. [13], corresponds to the maximum spin that can be generated

by aligning neutrons in the  $fp$  valence space. Shell-model calculations predict this state to be at about 1 MeV above the experimental value. On the other hand, a  $6^-$  state has been observed in  $^{64}\text{Ni}$  at excitation energy of 4172 keV. The coupling of the proton hole to the  $6^-$  state would give rise to a  $19/2^+$  state. Our calculations predict a  $19/2^+$  state in this energy region and therefore a positive-parity assignment would give a better agreement. We note that a positive-parity assignment was not explicitly excluded by Regan *et al.* in Ref. [13].

When approaching  $N = 40$ , excitations to the  $gd$  orbitals become important and, in fact, in  $^{65}\text{Co}$ , they are dominant in the wave function of all the calculated states. In Fig. 9 the experimental levels are compared with the shell-model results in the  $fpgd$  valence space. The agreement is good also for the high-spin states, but what is remarkable is that the inversion in energy of the  $9/2^-$  and  $11/2^-$  states with respect to the lighter odd-even cobalt isotopes is well reproduced.

The order of the  $9/2^-$  and the  $11/2^-$  states is closely bound to the mass quadrupole moment of the  $2^+$  phonon state of the even nickel core. This can be easily understood in the framework of the particle-vibrator weak-coupling scheme, where the energy splitting of the states in the multiplet can be





EXP

CALC

 $^{65}\text{Co}$ 

FIG. 10. Comparison between the calculated excitation energies of the  $2^+_{66\text{Ni}} \otimes \pi(f_{7/2})^{-1}$  multiplet members from the weak-coupling scheme (see text) and the experiment.

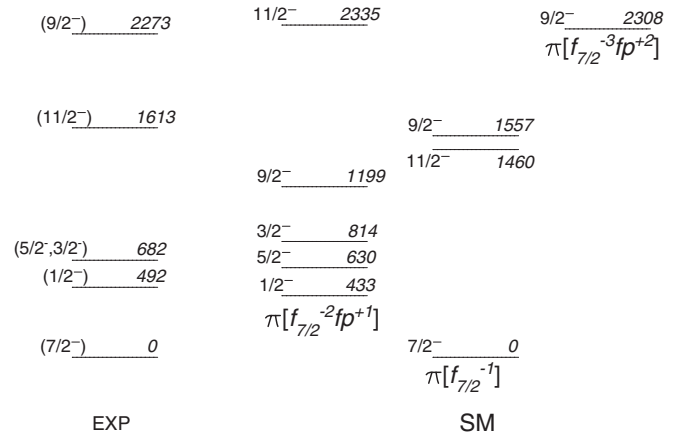
estimated to first order by means of the quadrupole-quadrupole interaction [34,35]

$$\Delta E(J) = k_2 \langle L \parallel Q \parallel L \rangle \langle j \parallel q \parallel j \rangle (-)^{j+L+J} \begin{Bmatrix} L & j & J \\ j & L & 2 \end{Bmatrix}, \quad (2)$$

where  $k_2$  is a coupling constant,  $Q$  is the mass quadrupole moment operator calculated for the vibrational core state, and  $q$  is the quadrupole moment of the proton  $(f_{7/2})^{-1}$  hole. It is clear that the order of the levels in the multiplet depends on the sign of the quadrupole moment of the  $2^+$  state in the even-even nickel. To illustrate the inversion of the  $9/2^-$  and the  $11/2^-$  states we report in Fig. 10 the comparison between the results obtained using Eq. (2) and the experimentally known levels belonging to the multiplet in  $^{65}\text{Co}$ . The calculations have been done as described in Ref. [35], by fixing the centroid of the multiplet at an energy value close to that of the  $2^+$  on  $^{66}\text{Ni}$  and using a positive quadrupole moment as a free parameter. Our shell-model calculations agree in predicting a positive quadrupole moment for  $^{66}\text{Ni}$ .

The  $^{67}\text{Co}$  nucleus is of particular interest since it corresponds to the magic  $N = 40$  number. It has therefore one proton less than the doubly-magic  $^{68}\text{Ni}$ , which has a spherical ground state, but only one proton more than  $^{66}\text{Fe}$ , which is a well-deformed nucleus. We thus expect to have coexistence of these two different structures at quite low-spin in  $^{67}\text{Co}$ .

The proposed level scheme for  $^{67}\text{Co}$  is reported in Fig. 11 in comparison with shell-model calculations in the  $fpgd$  space. Three different structures are predicted in the energy range of interest. The experimental  $(7/2^-)$  ground state and the  $(11/2^-)$  state at 1613 keV can be interpreted as a proton hole coupled to the g.s. and the  $2^+$  state in  $^{68}\text{Ni}$ , respectively. Also in this case the calculations give a positive quadrupole moment for the nickel core, which gives rise to the inversion of the  $9/2^-$  and  $11/2^-$  states. The shell model predicts a second  $9/2^-$  state only 100 keV above the energy of the  $11/2^-$  state with a structure compatible with that of the multiplet. The nonobservation of



EXP

SM

 $^{67}\text{Co}$ 

FIG. 11. Comparison of the experimental level scheme of  $^{67}\text{Co}$  with the results of large-scale shell-model calculations using the LNPS interaction.

such a state could be explained by the poor statistics obtained for this isotope.

On the other hand, the extrapolation of the systematics of the cobalt isotopes would suggest the assignment of  $9/2^-$  to the state at 2273 keV, close to the excitation energy of the  $2^+$  state in  $^{68}\text{Ni}$  (see Fig. 8). The calculations predict a third  $9/2^-$  state at 2308 keV, very close in energy to the one proposed at 2273 keV and with a similar decay pattern. This state is, however, not compatible with the multiplet interpretation as it presents a quite different structure that involves three proton holes in the  $f_{7/2}$  shell, but with a small deformation.

A third structure observed at low energy has been identified in Ref. [15] as having a configuration of two proton holes in the  $f_{7/2}$  shell and one proton-particle configuration in the Nilsson  $1/2^- [321]$  orbital. This deformed structure in our calculation arises from the excitation of four neutrons from the  $fp$  to the  $gd$  orbitals. This induces the reduction of the effective proton gap at  $Z = 28$ , giving rise to the  $1/2^-$  state at very low excitation energy. In the work of Pauwels *et al.* [15],  $J^\pi = (3/2^-)$  has been assigned to the state at 682 keV decaying through a 190-keV transition to the  $(1/2^-)$  isomer. The angular distribution that we measure for this transition is compatible with a pure  $E2$  transition or a mixed  $M1 + E2$  one, therefore not excluding the assignment of  $J^\pi = 5/2^-$  to the state above the isomer. This latter assignment would be in excellent agreement with the shell-model calculations as shown in Fig. 11. The spin of the state at 682 keV has been used to fix the spin and parity of the ground state of  $^{67}\text{Fe}$  in  $\beta$ -decay studies [36], and its determination is therefore important and deserves further experimental investigation. The theoretical  $3/2^-$  state is expected at higher excitation energy, consistent with a large decoupling parameter. The  $9/2^-$  state belonging to the deformed band built on the  $1/2^-$  state is predicted at 1199 keV, decaying to the  $5/2^-$  state with a transition of  $\sim 570$  keV. For all the states belonging to this band, the decay to the g.s. is precluded due to the very different structure. The calculated intrinsic quadrupole moment is very large,

$Q_0 \sim 180 \text{ e fm}^2$ , and stays constant for all the members of the rotational band. Experimentally, we observe few lines in the energy range of the expected in-band transitions, but the lack of  $\gamma$ - $\gamma$  coincidences does not allow their location in the level scheme.

The development of deformation in the mass region below  $^{68}\text{Ni}$  has been explained within the shell model in terms of the interplay between the evolution of the effective single-particle orbitals far from stability and the multipole correlations [19]. With two proton holes in the  $f_{7/2}$  shell,  $^{66}\text{Fe}$  presents a well-deformed ground state and is thus located in the island of inversion. For the nucleus  $^{68}\text{Ni}$ , having a spherical g.s., a deformed  $0_3^+$  state with a two proton–two hole configuration has been predicted [16] and recently reported at 2.2 MeV excitation energy [37]. In the nucleus  $^{67}\text{Co}$ , situated just between them, the deformed configuration comes very close to the ground state, at an excitation energy of 492 keV. It is remarkable that the shell-model calculations can account for such different coexisting structures. In these calculations up to eleven particle-hole excitations have been allowed across the  $Z = 28$  and  $N = 40$  gaps. The deformed  $1/2^-$  state gains about 5 MeV of correlation energy with respect to the ground state.

#### IV. SUMMARY AND CONCLUSIONS

In the present work the neutron-rich cobalt nuclei from  $A = 61$  to  $A = 67$  have been populated via multinucleon transfer reactions. The PRISMA magnetic spectrometer in conjunction with the CLARA Ge array at the INFN Laboratori Nazionali di Legnaro were used to identify the isotopes and to assign  $\gamma$  ray lines to them. New transitions have been observed in all the studied isotopes. In particular, for the most neutron rich isotopes the yrast states have been observed for the first time. The experimental findings have been discussed within large-scale shell-model calculations

performed using the newly developed interaction in the  $fpgd$  valence space. In general, most of the yrast levels of the odd-mass cobalt isotopes can be interpreted in terms of the weak coupling of the  $f_{7/2}$  proton hole to the excited states in the corresponding nickel cores. As  $N = 40$  is approached an increasing importance of neutron excitations to the  $g_{9/2}$  and  $d_{5/2}$  orbitals has been observed and this gives rise to the development of well-deformed structures. The coexistence of spherical and deformed structures at low excitation energy in  $^{67}\text{Co}$  are reproduced with extremely good precision by the shell-model calculations.

The evolution of these structures with increasing excitation energy is particularly interesting and would constitute a stringent test of the model. The present experimental setup precludes, however, the study of  $\gamma$ - $\gamma$  coincidences and therefore the construction of the level schemes on a solid basis. This will be possible in future thick-target experiments using a higher efficiency  $\gamma$  array, where the present recoil- $\gamma$  coincidences give the necessary input to construct the level schemes using multiple  $\gamma$  coincidences.

#### ACKNOWLEDGMENTS

The authors are grateful to the staff of the Tandem-ALPI accelerator of LNL for the excellent technical support received. This work was partially supported by the European Community FP6, Structuring the ERA Integrated Infrastructure Initiative Contract No. EURONS RII3-CT-2004-506065, by MICINN, Spain (Contract No. FPA2011-29854), by IN2P3, France (Contract No. AIC-D-2011-648), by Comunidad de Madrid, Spain (Contract No. HEPHACOS S2009-ESP-1473), and by Generalitat Valenciana, Spain (Contract No. PROMETEO/2010/101). A. Gadea and E. Farnea acknowledge the support of MICINN, Spain, and INFN, Italy, through the AIC-D-2011-0746 bilateral action.

- 
- [1] R. Broda *et al.*, *Phys. Rev. Lett.* **74**, 868 (1995).
  - [2] J. I. Prisciandaro *et al.*, *Phys. Lett. B* **510**, 17 (2001).
  - [3] W. Rother *et al.*, *Phys. Rev. Lett.* **106**, 022502 (2011).
  - [4] A. Gade *et al.*, *Phys. Rev. C* **81**, 051304 (2010).
  - [5] R. Grzywacz *et al.*, *Phys. Rev. Lett.* **81**, 766 (1998).
  - [6] R. Broda, *J. Phys. G* **32**, R151 (2006).
  - [7] N. Mărginean *et al.*, *Phys. Lett. B* **633**, 696 (2006).
  - [8] S. Lunardi *et al.*, *Phys. Rev. C* **76**, 034303 (2007).
  - [9] J. J. Valiente-Dobon *et al.*, *Phys. Rev. C* **78**, 024302 (2008).
  - [10] J. J. Valiente-Dobon *et al.*, *Phys. Rev. Lett.* **102**, 242502 (2009).
  - [11] S. Szilner *et al.*, *Phys. Rev. C* **84**, 014325 (2011).
  - [12] D. Montanari *et al.*, *Phys. Lett. B* **697**, 288 (2011).
  - [13] P. H. Regan, J. W. Arrison, U. J. Huttmeier, and D. P. Balamuth, *Phys. Rev. C* **54**, 1084 (1996).
  - [14] H. Junde, *Nucl. Data Sheets* **109**, 787 (2008).
  - [15] D. Pauwels *et al.*, *Phys. Rev. C* **78**, 041307 (2008).
  - [16] D. Pauwels *et al.*, *Phys. Rev. C* **79**, 044309 (2009).
  - [17] A. Dijon *et al.*, *Phys. Rev. C* **83**, 064321 (2011).
  - [18] E. Caurier, F. Nowacki, and A. Poves, *Eur. Phys. J. A* **15**, 145 (2002).
  - [19] S. M. Lenzi, F. Nowacki, A. Poves, and K. Sieja, *Phys. Rev. C* **82**, 054301 (2010).
  - [20] M. Hannawald *et al.*, *Phys. Rev. Lett.* **82**, 1391 (1999).
  - [21] N. Aoi *et al.*, *Phys. Rev. Lett.* **102**, 012502 (2009).
  - [22] J. Ljungvall *et al.*, *Phys. Rev. C* **81**, 061301 (2010).
  - [23] A. Gadea *et al.*, *Eur. Phys. J. A* **20**, 193 (2004).
  - [24] A. M. Stefanini *et al.*, *Nucl. Phys. A* **701**, 217c (2002).
  - [25] S. Szilner *et al.*, *Phys. Rev. C* **76**, 024604 (2007).
  - [26] D. Montanari *et al.*, *Eur. Phys. J. A* **47**, 4 (2011).
  - [27] D. Montanari *et al.*, *Phys. Rev. C* **85**, 044301 (2012).
  - [28] C. Rossi Alvarez, *Nucl. Phys. News* **2**, 10 (1993).
  - [29] U. Bosch *et al.*, *Nucl. Phys. A* **477**, 89 (1988).
  - [30] M. Block *et al.*, *Phys. Rev. Lett.* **100**, 132501 (2008).
  - [31] H. Junde and B. Singh, *Nucl. Data Sheets* **91**, 317 (2000).
  - [32] M. Asai, T. Ishii, A. Makishima, I. Hossain, M. Ogawa, and S. Ichikawa, *Phys. Rev. C* **62**, 054313 (2000).
  - [33] A. P. Zuker, J. Retamosa, A. Poves, and E. Caurier, *Phys. Rev. C* **52**, R1741 (1995).
  - [34] L. Trache, A. Kolomiets, S. Shlomo, K. Heyde, H. Dejbakhsh, C. A. Gagliardi, R. E. Tribble, X. G. Zhou, V. E. Iacob, and A. M. Oros, *Phys. Rev. C* **54**, 2361 (1996).
  - [35] A. de-Shalit, *Phys. Rev.* **122**, 1930 (1961).
  - [36] J. M. Daugas *et al.*, *Phys. Rev. C* **83**, 054312 (2011).
  - [37] A. Dijon *et al.*, *Phys. Rev. C* **85**, 031301 (2012).